Supplemental Material

Developmental timing of programmed DNA elimination in *Paramecium tetraurelia* recapitulates germline transposon evolutionary dynamics

Coralie Zangarelli, Olivier Arnaiz, Mickaël Bourge, Kevin Gorrichon, Yan Jaszczyszyn, Nathalie Mathy, Loïc Escoriza, Mireille Bétermier, Vinciane Régnier

Correspondence: Mireille Bétermier, Vinciane Régnier

Email: mireille.betermier@i2bc.paris-saclay.fr; vinciane.regnier@i2bc.paris-saclay.fr

This PDF file includes:

Supplemental Methods

Transformation of the 51 *nd7-1* strain

A complementing plasmid carrying a functional *ND7* gene was microinjected into the MAC of vegetative 51 *nd7-1* cells to allow for easy screening of transformant clones (Dubois et al. 2017). The complementing *ND7* transgene (Tg *ND7*) bears a silent Single Nucleotide Polymorphism (SNP) (T->C scaffold 51_5: 596316) compared to the endogenous gene (designated as endo *ND7*). Transgene injection levels (Copy Per Haploid Genome or CPHG) were determined by qPCR on genomic DNA extracted from vegetative transformants, using a LightCycler 480 and the LightCycler 480 SYBR green Master Kit (Roche Diagnostics). Two pairs of oligonucleotide primers (5'TTCCAAGGACCCTGCATAAT3'/5'GGACTGAACCAGAGCCTTCA3') and *(*5'AGCTCCTGATGGCAAGACAT3'/5'AGTCTGTCCACAACCAGCTG3') were used to amplify the *ND7* transgene and genomic *KU80c* reference locus, respectively.

Contribution of contaminating old MAC fragments to sorted new MAC DNA

We used FANS to sort nuclei from the Tg *ND7* clone at the DEV2 stage (Supplemental Fig. S3B) and deep-sequenced the DNA extracted from three sorted populations (new MACs, peak 1; new MACs, peak 2; fragments) (tc3 in Supplemental Tables S1, S2**).** For each sample, we experimentally determined the ratio Tg *ND7*/endo *ND7*. For old MAC fragments, this ratio is equal to the transgene CPHG of the parental microinjected clone ($CPHG_{FRAG}$). For the new MAC samples, because sorted new MAC DNA contains DNA from contaminating old MACs, this ratio represents the apparent transgene CPHG ($CPHG_{app}$). For each sample, we counted the copies of the *ND7* locus from Tg *ND7* and/or endo *ND7* and defined the % of contamination as follows:

% Contamination = (endo $ND7_{FRAG}$/ endo $ND7_{sample}$) x100

with:

endo $ND7_{FRAG}$ = Tg *ND7*/ $CPHG_{FRAG}$

endo $ND7_{sampl\ e}$= Tg *ND7*/ $CPHG_{app}$

which gives:

% Contamination = $CPHG_{app}/CPHG_{FRAG}$

We used three independent methods to calculate the transgene CPHG values (Supplemental Fig. S3C). In the first method (qPCR), CPHG values were calculated from a qPCR performed on sequencing libraries using the *ND7* transgene and *KU80c* oligonucleotide primers. In the second method, the SNP present in the *ND7* transgene was used to quantify the number of sequencing reads coming from the endogenous *ND7* locus or from the Tg *ND7* transgene. The ratio between the number of Tg and endo *ND7* reads gives the transgene CPHG in each sample. The third method used genomic read coverage calculated with bamCoverage (v3.2.1 --binsize 20 --smoothlength 50 --region scaffold51_5:592000:598000). The ratio between the mean coverage of the *ND7* gene (594873-596396) and the mean coverage of its upstream region (592000-594000), minus 1 gives the transgene CPHG in each sample. Contamination levels within the range of 0.9-6.1% and 1.1-4.7% were obtained for the first and second DNA peaks, respectively, indicative of the high purity of the sorted anlagen.

Annotation of IESs in MIC-limited regions

The MIC-limited genome consists of IESs as well as regions that are imprecisely eliminated. We looked for additional IESs inside each compartment. The ParTIES MILORD module was used to identify frequent non-canonical excision events. Events inside an annotated IES were designated “internal IESs” and events in imprecisely eliminated MIC-limited regions were designated “buried IESs”. “internal IESs” were annotated using the MAC+IES reference genome (scaffolds > 30 kb). Only internal and partial internal deletion events bounded by two TAs were considered (see Supplemental Fig. S7A). A series of filters (minimum size 20 nt; no coverage of the event in FRAG samples; events must be revealed by at least 10 reads in at least 2 time course samples; only the event supported by the maximum number of reads is kept in the case of overlapping events) were applied to provide a list of 226 putative internal IESs. The 167 buried IESs were annotated using the MIC reference genome (contigs > 1 kb) and reads that do not map on the MAC or the MAC+IES reference genomes, to select deletion events (length < 5 kb) localized in imprecisely eliminated MIC-limited regions. The same filters used for internal IES identification were applied.

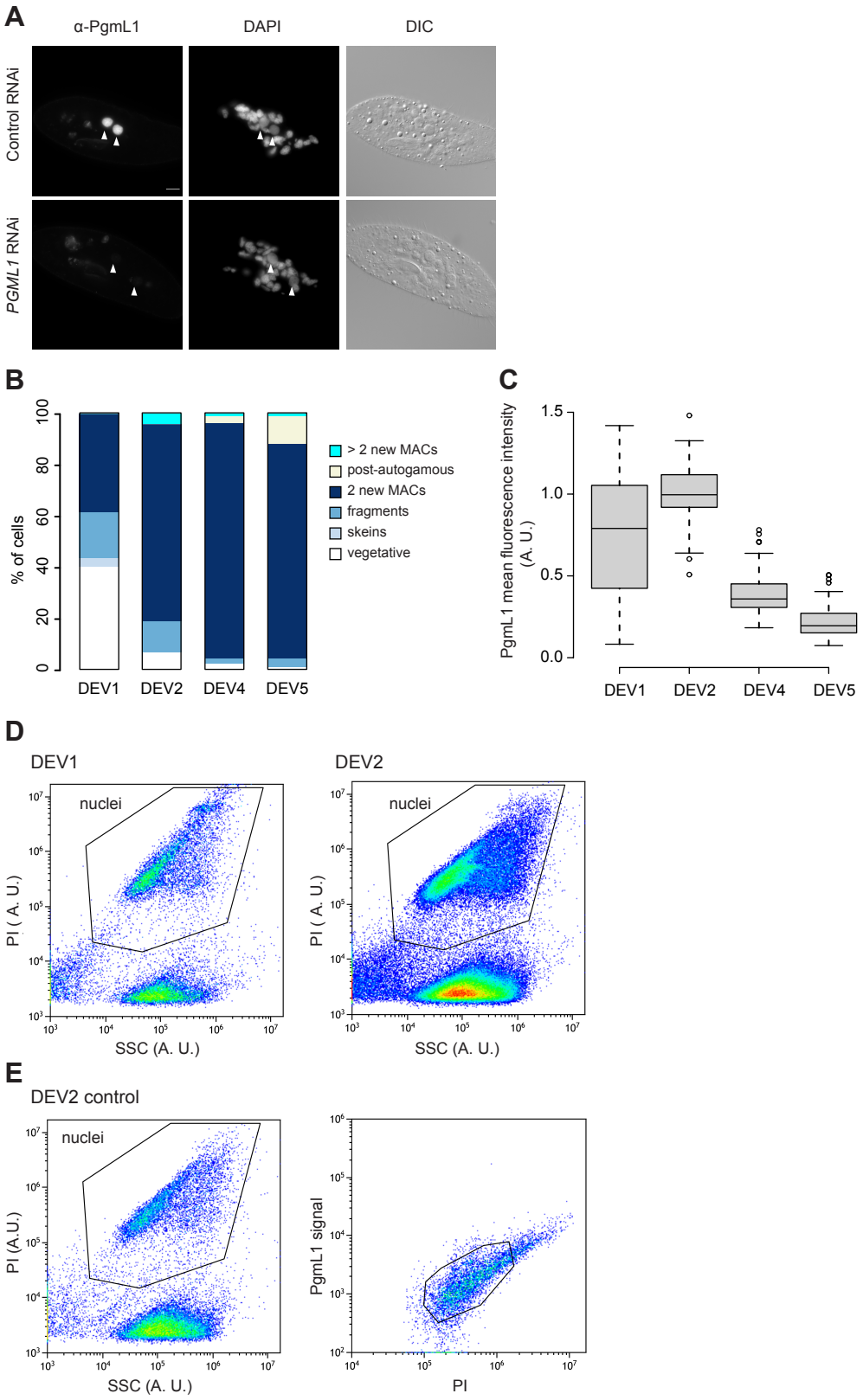

Supplemental Fig. S1. PgmL1 immunostaining on whole cells and isolated nuclei during developmental time-courses. (*A*) Validation of the specificity of the α-PgmL1 antibody. Immunostaining of PgmL1 in DEV2 autogamous cells subjected to control or *PGML1* RNAi. (*B*) Cytological progression of autogamy time-course tc1. For each developmental stage (DEV1: T3; DEV2: T10; DEV4: T30; DEV5: T48; with time in hours following T0), the percentage of cells with a defined cytological status (see legend) was determined following DAPI staining of fixed cells and fluorescence microscopy. >2 new MACs stands for cells with 3 or more new MACs. (C) Boxplot representation of the distribution of PgmL1 fluorescence intensities at the different stages of tc1. 78 to 88 labeled new MACs were quantified at each stage. (D) Flow cytometry analysis of immunostained nuclei in tc2. Gating of total nuclei from DEV1 and DEV2 based on their PI and Side Scatter (SSC) signals. (E) Same experiment as in *D* at DEV2 stage without adding the α-PgmL1 primary antibody. A. U.: arbitrary units.

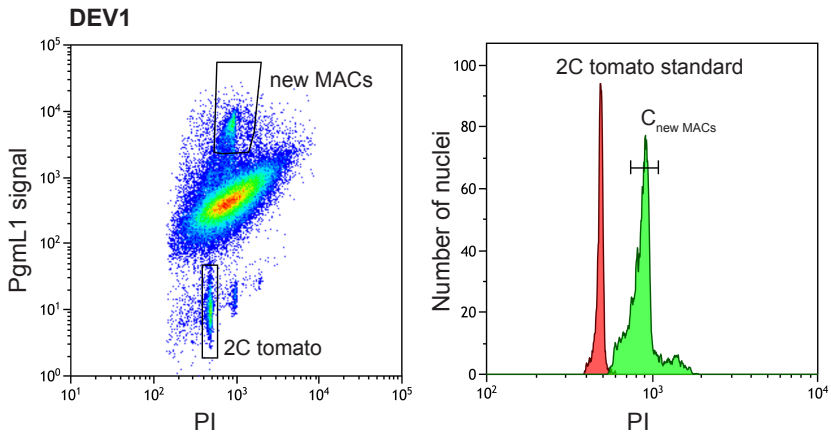

Supplemental Fig. S2. Example of C-value estimation for sorted new MAC populations. Tomato nuclei were added to *Paramecium* nuclei isolated at the DEV1 stage from tc4 as shown on the PgmL1 vs PI plot. Peaks of DNA content are defined on the PI histogram. The observed mean PI fluorescence for 2C tomato nuclei is used as an internal standard to calculate the C-value for the DEV1 new MAC population.

A

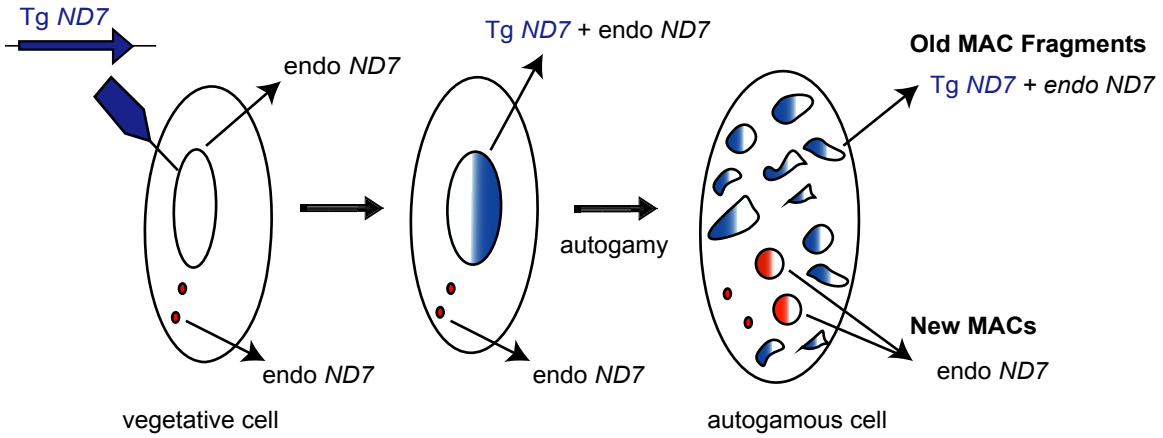

B

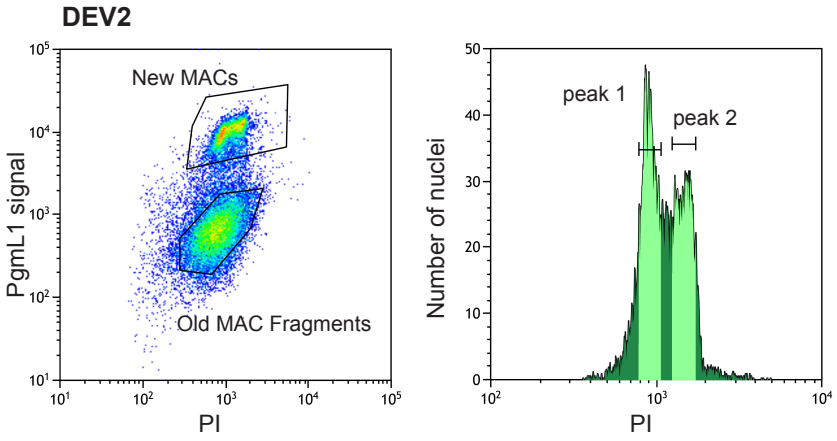

C

		Fragments	New MACs, peak 1	New MACs, peak 2
qPCR	CPHG	183.8	1.6	2
	contamination (%)		**0.9**	**1.1**
ND7 SNP	Reads endo *ND7*	103	115	124
	Reads Tg *ND7*	6198	420	352
	CPHG	60.2	3.7	2.8
	contamination (%)		**6.1**	**4.7**
ND7 coverage	*ND7* upstream coverage	94.9	120.5	153.9
	ND7 coverage	9438	654.5	604.4
	CPHG	98.5	4.4	2.9
	contamination (%)		**4.5**	**3**

Supplemental Fig S3. Determination of the contamination level of sorted new MACS with old MAC fragments. (*A*) Schematic representation of the strategy used. A *Paramecium* clone carrying Tg *ND7* in its somatic MAC was generated by microinjection and starved to induce autogamy. The presence of Tg *ND7* in the DNA isolated from sorted new MACs makes it possible to calculate the contamination by old MAC fragments as described in Supplemental Methods. (*B*) Flow cytometry sorting of nuclei from the Tg *ND7* clone at the DEV2 stage of an autogamy time-course (tc3). Gated events are indicated. Sorted new MAC peaks (1 and 2) are indicated by a light green shading on the PI histogram. Old MAC fragments, sorted as a control, are indicated on the PgmL1 vs PI plots. (*C*) Calculation of the contamination level of purified new MAC DNA from the Tg *ND7* clone. Of note, the qPCR-based method yielded lower contaminating values than the sequencing read counts.

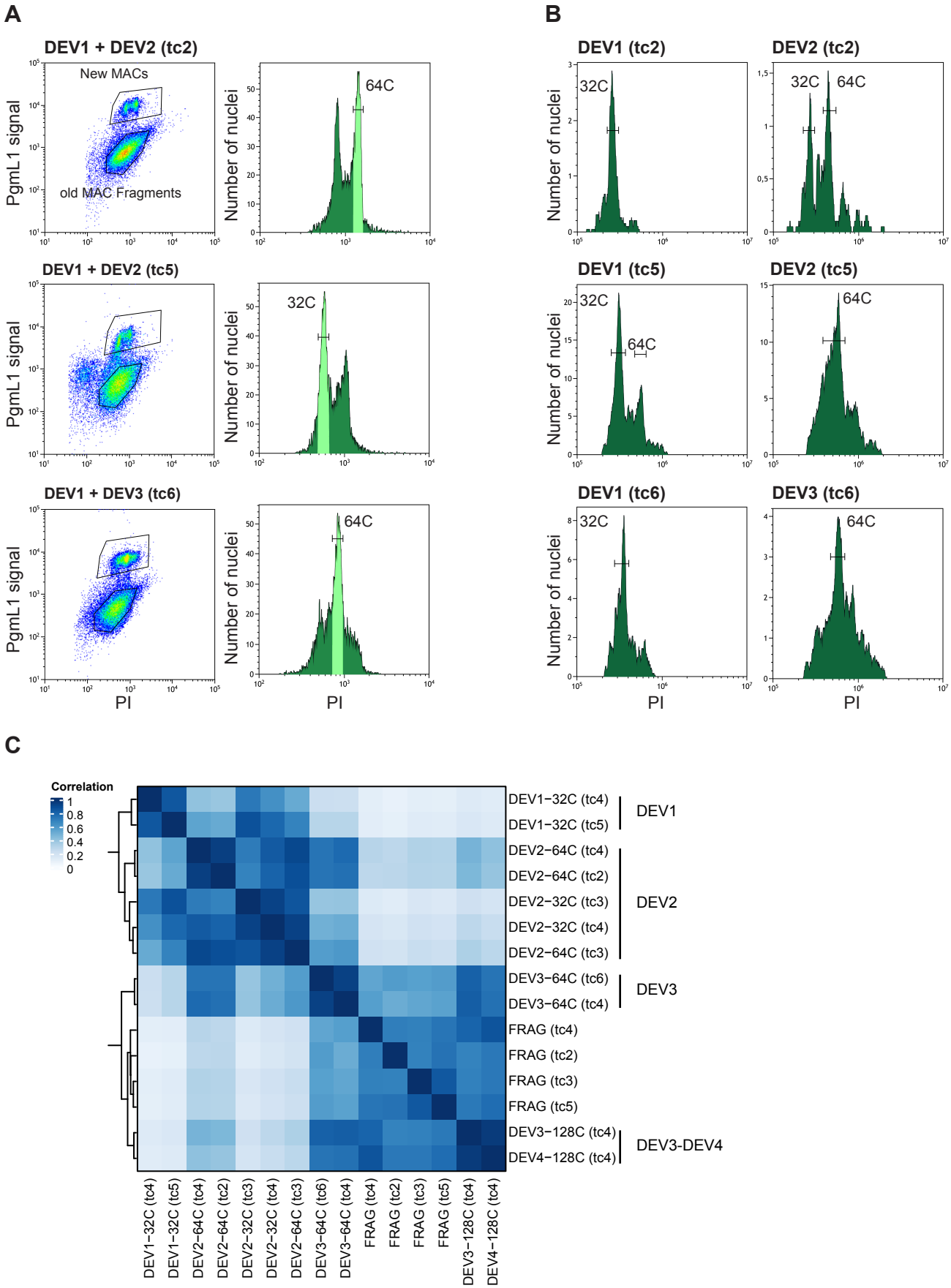
A
DEV1 + DEV2 (tc2)
New MACs
old MAC Fragments
PgmL1 signal
Number of nuclei
64C
DEV1 + DEV2 (tc5)
32C
DEV1 + DEV3 (tc6)
PI
B
DEV1 (tc2)
DEV2 (tc2)
32C
64C
DEV1 (tc5)
DEV2 (tc5)
DEV1 (tc6)
DEV3 (tc6)
C
Correlation
1
0.8
0.6
0.4
0.2
0
DEV1−32C (tc4)
DEV1−32C (tc5)
DEV2−64C (tc4)
DEV2−64C (tc2)
DEV2−32C (tc3)
DEV2−32C (tc4)
DEV2−64C (tc3)
DEV3−64C (tc6)
DEV3−64C (tc4)
FRAG (tc4)
FRAG (tc2)
FRAG (tc3)
FRAG (tc5)
DEV3−128C (tc4)
DEV4−128C (tc4)
DEV1
DEV2
DEV3
DEV3-DEV4

Supplemental Fig. S4. Replicate flow cytometry experiments. (*A*) Flow cytometry sorting for tc2, tc5 and tc6. The sorting was performed on a pool of nuclei isolated from 2 developmental stages (DEV1 + DEV2 or DEV1 + DEV3). Gated events are indicated. Sorted peaks are indicated by light green shading on the PI histogram. In each case, the sorted new MAC peaks correspond to a unique developmental stage as shown in the analytical flow cytometry presented in *B*. Estimation of the C-level for the indicated peaks is presented in Supplemental Table S1. The sorted old MAC fragments, used as controls, are indicated on the PgmL1 labelling vs PI plots. (*B*) Flow cytometry analysis for tc2, tc5, and tc6. The PI histogram of PgmL1-labelled nuclei is presented for each developmental stage analyzed individually. Estimation of the C-level for each peak was performed using tomato nuclei as an internal standard, as for sorting experiments. (*C*) Pearson correlation matrix of IES excision scores between samples. The correlation is encoded from 0 (light blue) to 1 (dark blue). The hierarchical clustering between samples is indicated on the left.

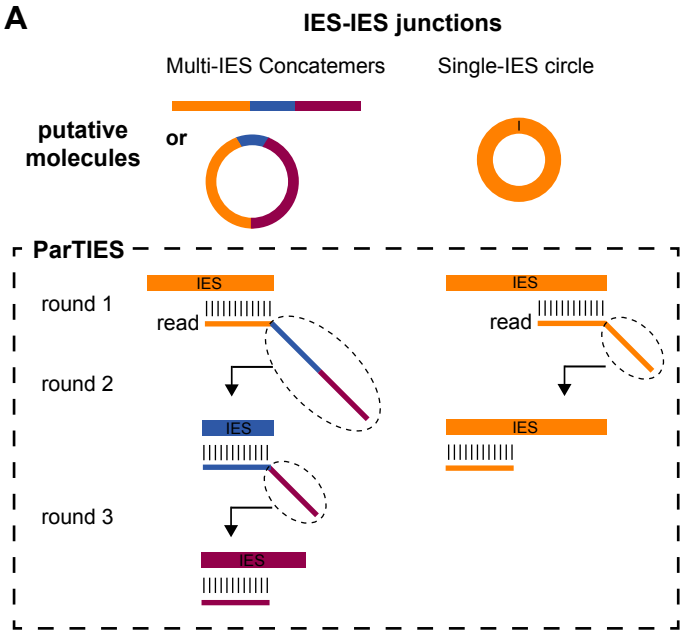

B

	Samples	Multi-IES concatemers	Single-IES circles	% of single-IES circles
	FRAG tc2	1.56	0	**0**
	tc3	10.73	0.06	**0.6**
	tc4	5.46	0	**0**
	tc5	4.90	0.02	**0.5**
32C	DEV1 tc4	355.71	0.06	**0**
	tc5	708.93	0.65	**0.1**
	DEV2 tc3	1127.04	4.21	**0.4**
	tc4	1608.79	1.18	**0.1**
64C	tc3	1006.11	7.87	**0.8**
	tc4	188.66	1.97	**0.2**
	tc2	876.10	14.37	**1.6**
	DEV3 tc6	389.98	6.68	**1.7**
	tc4	370.58	2.62	**0.7**
128C	DEV3 tc4	54.63	1.28	**2.3**
	DEV4 tc4	34.80	0.82	**2.3**

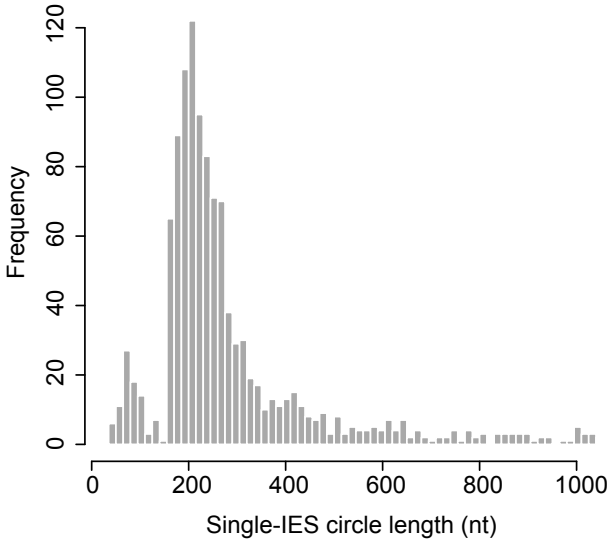

Supplemental Fig. S5. Detection of IES-IES junctions. (*A*) Schematic representation of the bioinformatic method used for the detection of IES-IES junctions. The ParTIES concatemer module was developped to detect multi-IES concatemers and single-IES circles, using reads mapped recursively on IES sequences. The procedure is schematically presented in the box and described in Methods. (*B*) Normalized number of sequencing reads (RPM) corresponding to the two types of molecules (multi-IES concatemers or single-IES circles) resulting from the ligation of excised IES ends (see schematic representation in *A*). Linear or circular concatemers cannot be distinguished with Illumina sequencing. (*C*) Size distribution of IESs involved in at least one single-IES circle.

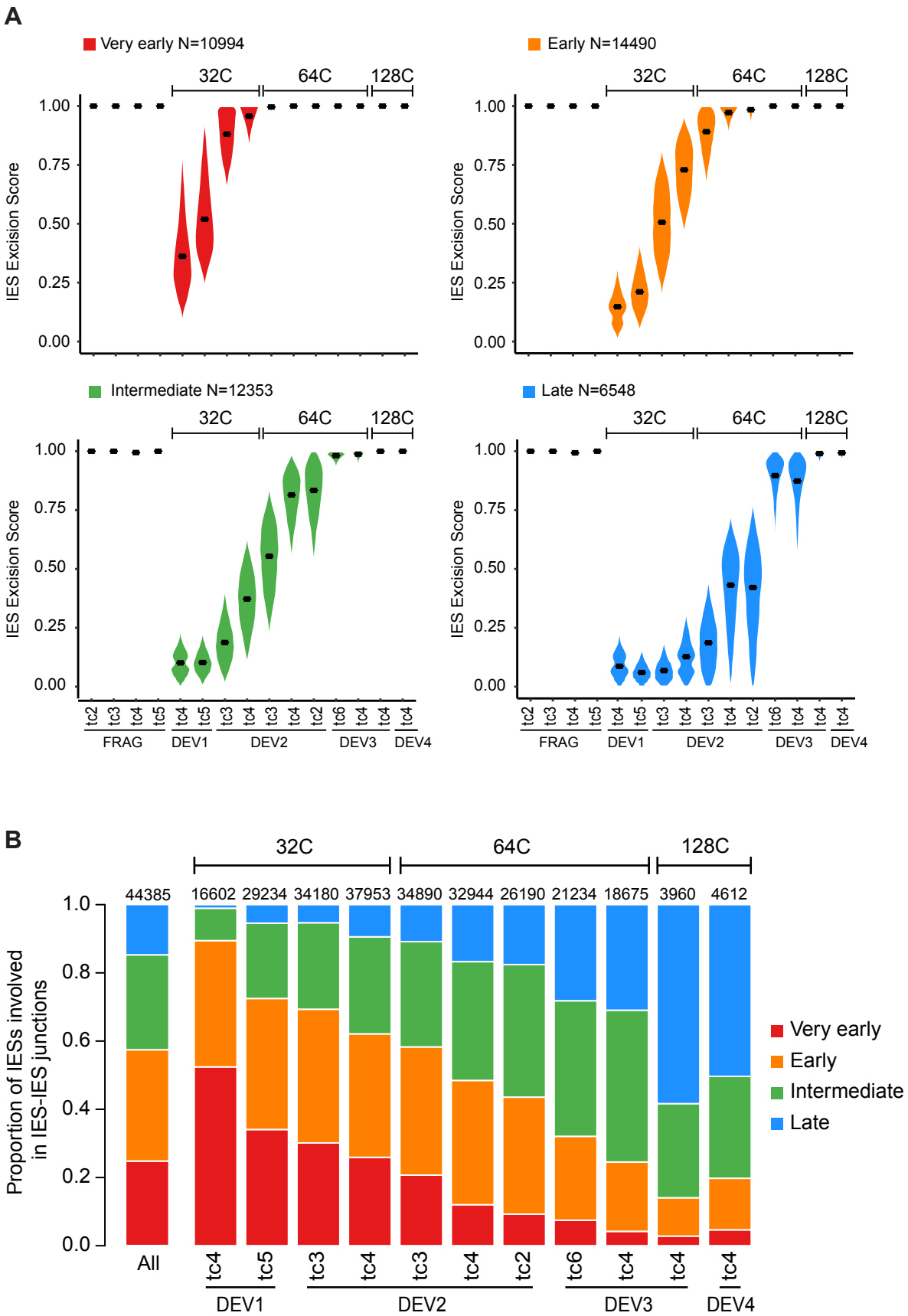

Supplemental Fig S6. Detection of excision products. (*A*) ES distribution in each sample for each excision profile group. (*B*) Proportion of IESs involved in at least one excised IES-IES junction in the four excision profile groups (indicated by colors). "All" is the random expectation for all IESs. The number of IESs in each dataset is indicated above each bar.

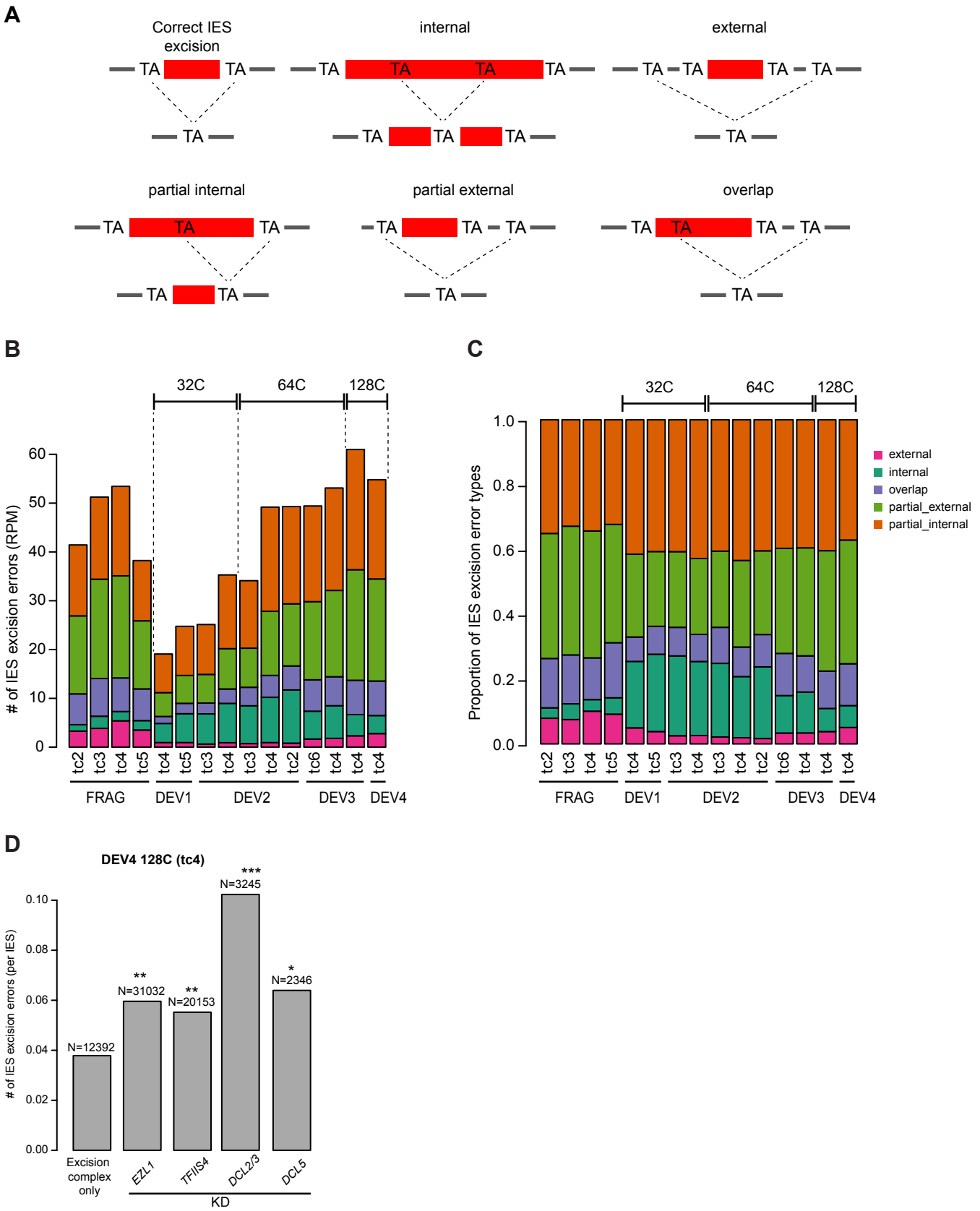

Supplemental Fig. S7. Detection of IES excision errors. (*A*) Schematic representation of IES excision errors. In internal or external errors, the two alternative TAs are misplaced: inside or on each flanking side of the reference IES, respectively. Partial internal and partial external excision errors use one correct TA boundary and the other TA inside or outside of the reference IES, respectively. Overlapping error uses one TA inside and the other outside of the reference IES. (*B*) Normalized counts (per million mapped reads) of excision errors in the different sorted new MAC population or in fragments. (*C*) Proportion of the different types of excision errors. (D) Abundance of IES excision errors in datasets of epigenetically-controlled IESs. The frequencies of IES excision errors for each dataset are compared to the frequency observed for IESs that belong to the group “excision complex only” using a chi-square statistical test (p-values: *<1e-5; **<1e-10; ***<1e-40).

A

IES group	Genes (%)	P-value	CDS (%)	P-value	Introns (%)	P-value
All	84.5	-	76	-	5.4	-
Very early	90.3	6.7e-55	82.6	1e-49	5.1	0.2
Early	88.4	1.4e-31	79.4	1.4e-17	5.8	0.1
Intermediate	83.9	0.1	74.9	0.01	5.7	0.3
Late	72.1	2.9e-138	63.8	6.6e-100	4.9	0.1

B

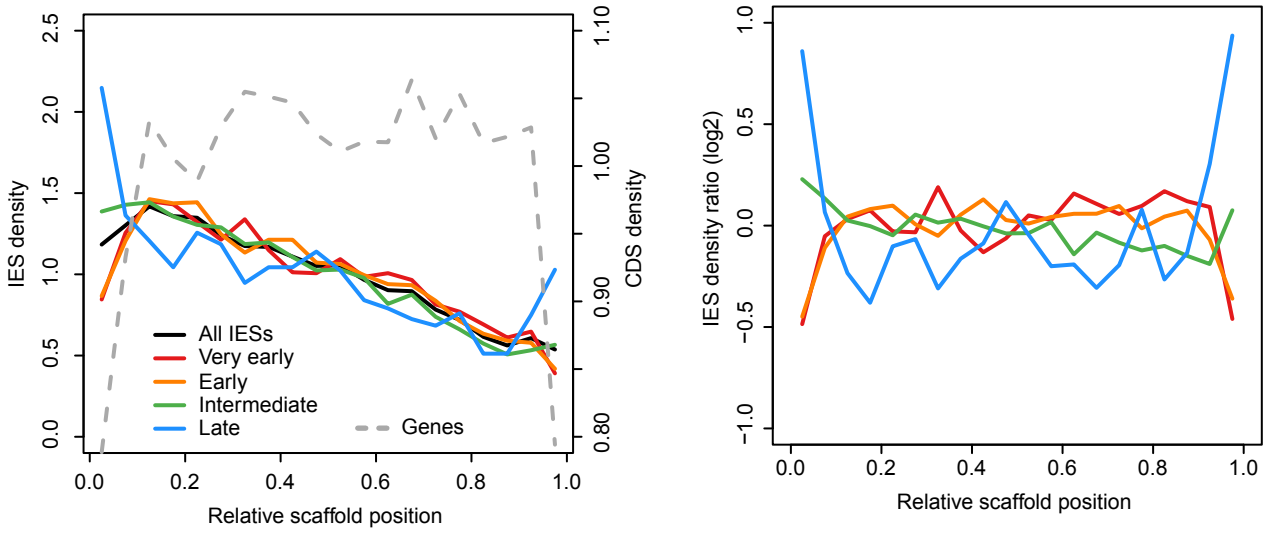

Supplemental Fig. S8. IES location for excision profile groups. (*A*) Table showing the percentages of IESs in genes, coding sequences (CDS) and introns for all IESs and for IESs belonging to each group. A chi2 test was performed to compare the proportion obtained in each group with the proportion for all IESs, and the associated p-values are presented. (*B*) IES density along scaffolds. Relative densities for IES site location were calculated (bin of 0.05) on the 117 scaffolds with telomeres at both ends (Duret et al. 2008), previously oriented to have higher IES density on the first left quarter of the scaffold. Gene density was calculated using the same method and the middle position of each coding exon. Left panel: the gray dotted line shows gene density and the black curve shows IES density. The red, orange, green and light blue curves show the IES density for the 4 groups of excision profiles. Right panel: ratio between IES density for each group relative to the total IES density.

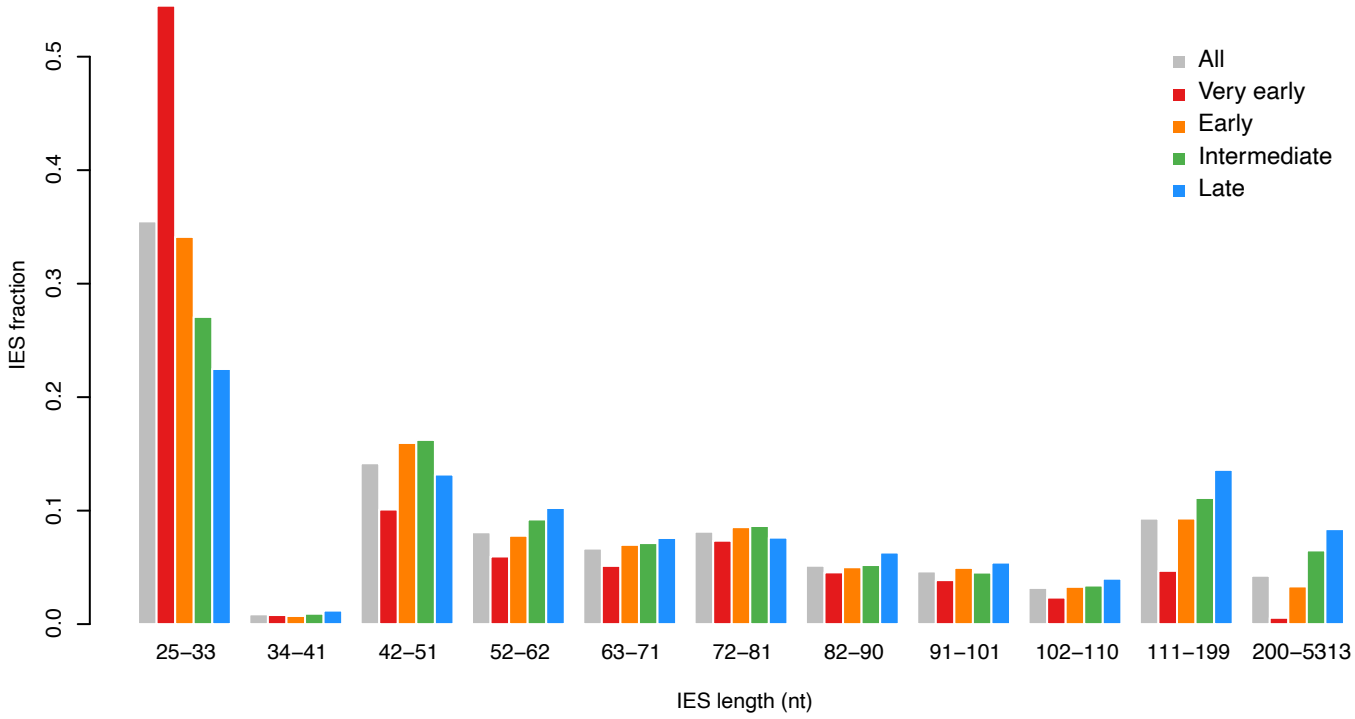

Supplemental Fig. S9. IES fraction in each peak of IES length, for all IESs (gray) and for IESs belonging to the four excision profile groups.

A

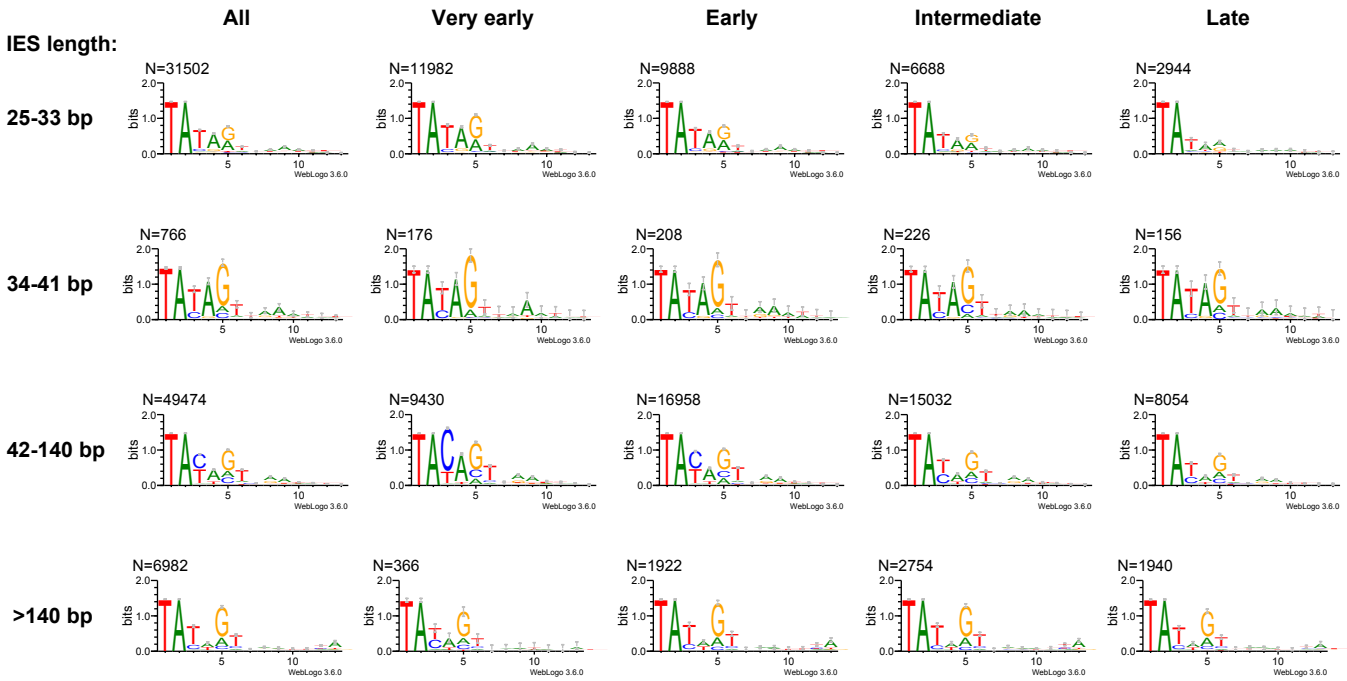

B

	pos.	base	All	Very early	Late
25-33 bp	3	T	79%	82%**	72%
	4	A	76%	82%**	65%
	5	G	52%	62%***	35%
42-140 bp	3	C	49%	77%****	30%
	4	A	73%	88%***	62%
	5	G	60%	64%	57%

Supplemental Fig. S10. Analysis of IES ends. (*A*) Sequence logos of IES ends, calculated according to the IES size (rows) and excision profile group (columns). The first column is for all IESs. (*B*) Base frequencies at positions 3, 4, 5 of IES ends for all, very early and late IESs from the 25-33 bp and 42-150 bp length categories. The frequencies for very early and late IESs were compared using a statistical test using a binomial frequency test (binom.test) and a Pearson-Klopper exact method to calculate the upper bound of the confidence interval (binom.confint with the parameters conf.level=0.95). Resulting p-values were adjusted for multiple testing using the Benjamini & Hochberg method. Frequencies with a p-value < 0.001 are considered as statistically significant (p-values: * <= 1e-50; ** <1e-100; *** < 1e-300; **** < 1e-400).

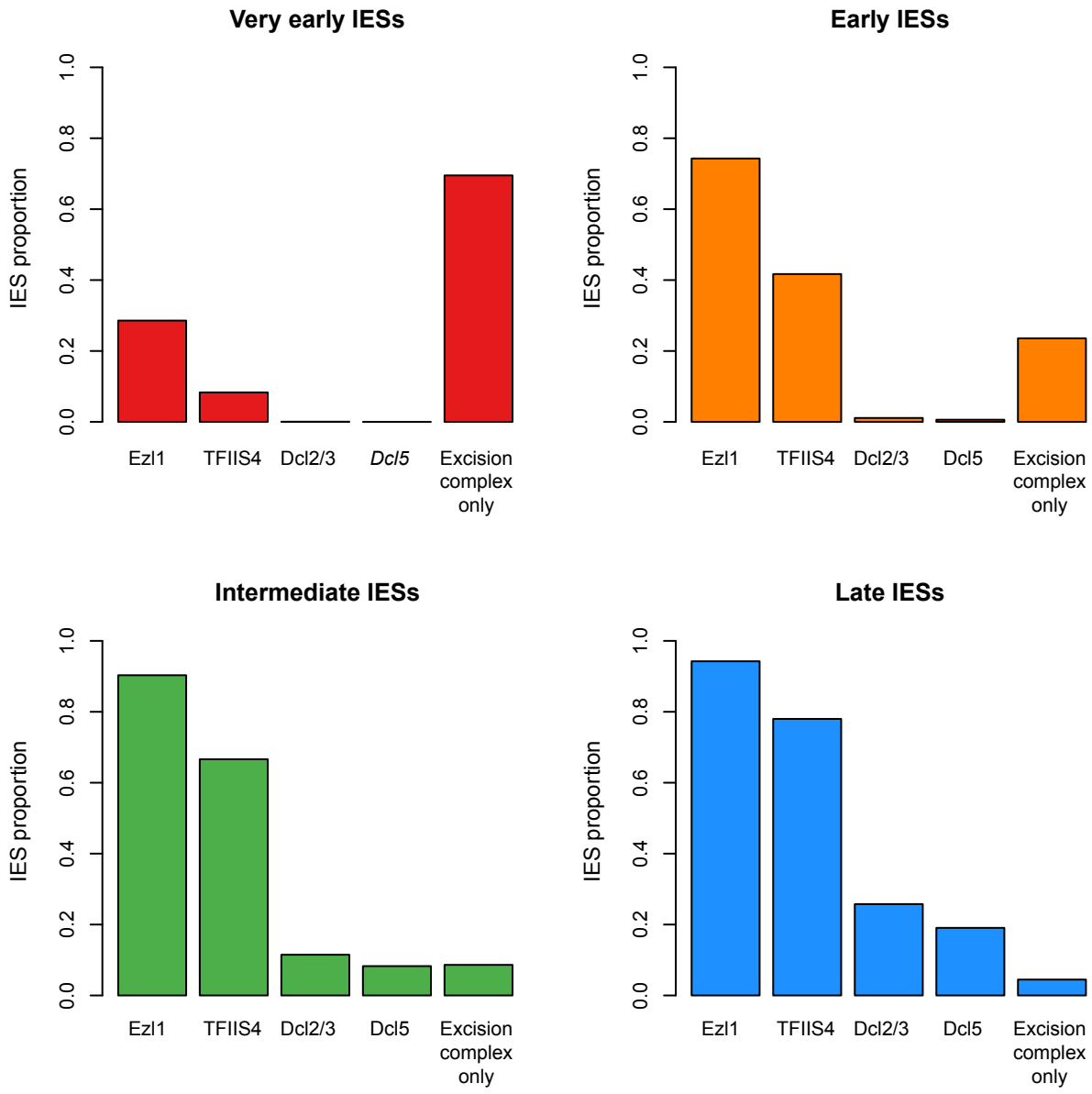

Supplemental Fig. S11. Proportion of Ezl1, TFIIS4, Dcl2/3 or Dcl5-dependent IESs compared to the proportion of IESs only dependent upon Pgm (labelled "excision complex only"). Each excision profile group is represented in a separate panel.

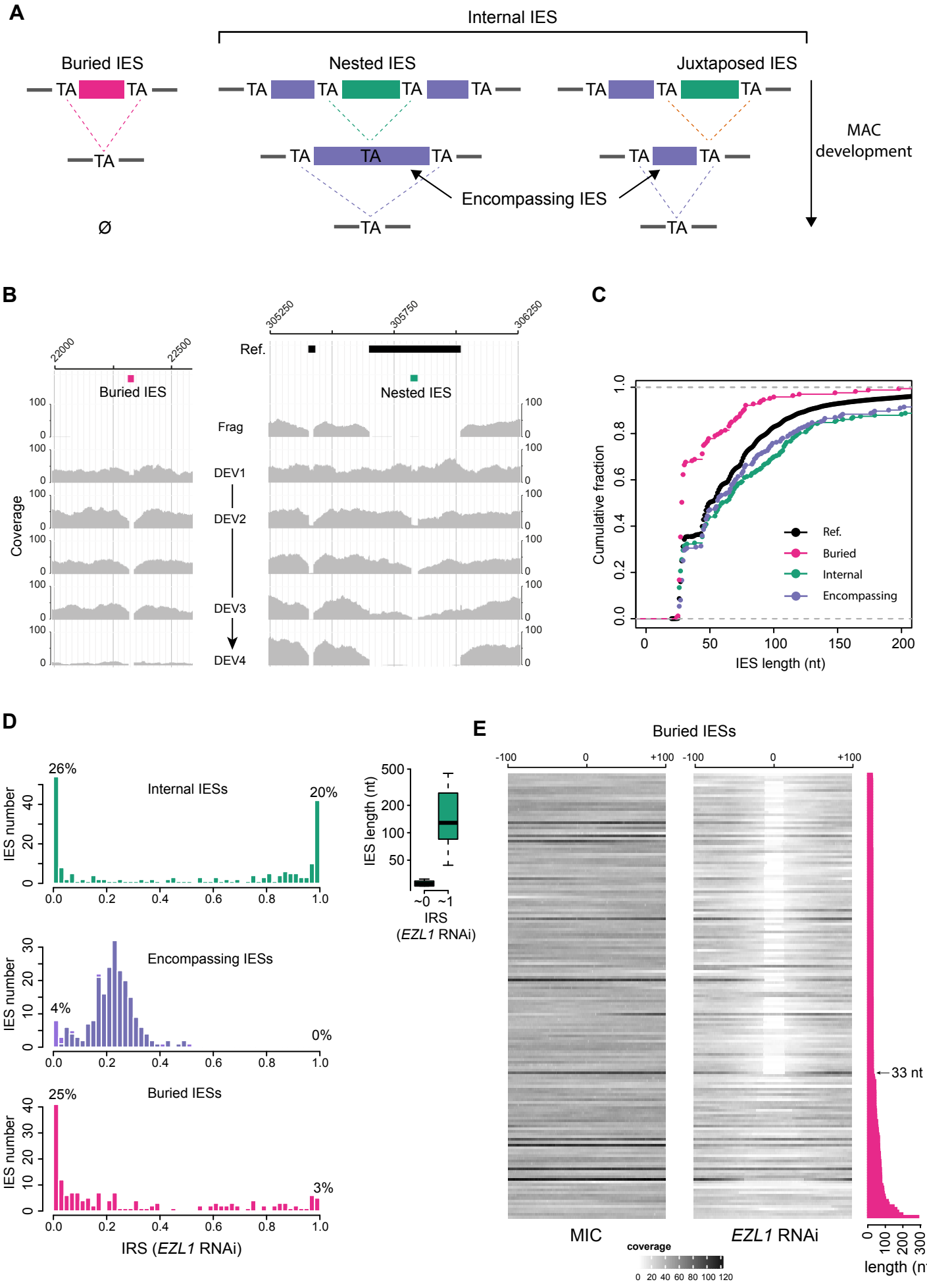
A
Internal IES
Buried IES
Nested IES
Juxtaposed IES
TA
MAC development
Encompassing IES
Ø
B
Buried IES
Nested IES
Ref.
Frag
DEV1
DEV2
DEV3
DEV4
Coverage
C
Cumulative fraction
IES length (nt)
Ref.
Buried
Internal
Encompassing
D
Internal IESs
Encompassing IESs
Buried IESs
IES number
IES length (nt)
IRS (EZL1 RNAi)
26%
20%
4%
0%
25%
3%
E
Buried IESs
MIC
EZL1 RNAi
coverage
33 nt
length (nt)

F

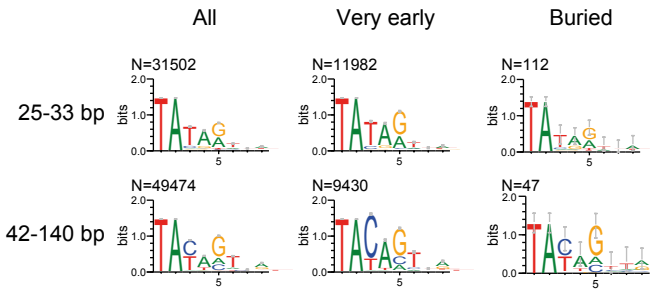

Supplemental Fig. S12. Annotation and properties of IESs localized in MIC-specific regions. (*A*) Schematic representation of excision events transiently observed during MAC development. These newly characterized TA-bound IESs can be of two types: IESs localized in imprecisely eliminated regions that will be completely removed from the mature MAC (buried IES) or sequences localized within an IES of the reference set (internal IES). In the latter case, two situations can be distinguished depending on whether the new IES is excised between fully internal TAs (nested IES) or shares one TA with its encompassing IES (juxtaposed IES). (*B*) Genome browser screenshots showing one buried IES (left panel, genome location: NODE_7045_length_27888_cov_20.982180:22000-22500) and one nested IES (right panel, genome location: scaffold51_106_with_IES: 305250-306250) that was already described inside IES 51A6649 from the A^{51} surface antigen gene. The histogram tracks correspond to the sequencing coverage in the sorted samples from the tc4 time-course (DEV1 32C, DEV2 32C, DEV2 64C, DEV3 64C, DEV4 128C). (*C*) Cumulative fraction of the characterized IES datasets according to their length (nt). Ref.: reference set of IESs; Buried: buried IESs; Internal: internal IESs (nested or juxtaposed); Encompassing: encompassing IESs. (*D*) Histogram distributions (bin 0.02) of IES Retention Scores (IRS) in *EZL1* RNAi for IESs belonging to the following categories: buried (N=167), internal (N=226), encompassing (N=223). Only IESs with an IRS calculated from at least 10 reads are displayed (N=164, 209, 223 respectively). The percentage of IESs for the two extreme bins (IRS around 0 and IRS around 1) of the distribution are indicated above the bars. For internal IESs, the length distribution is added as a boxplot for these two IRS categories. (*E*) Heatmaps of coverage within a 200-nt window around buried IESs (0 being the center of each buried IES) for a vegetative MIC DNA sample (left) (Sellis et al. 2021) and DNA after *EZL1* RNAi (right) (Lhuillier-Akakpo et al. 2014). IESs, on each row, have been ordered according to their lengths, as illustrated on the pink histogram. The gray scale color intensity corresponds to sequencing depth coverage. (*F*) Sequence logos of the 8 bases at IES ends for all IESs, IESs belonging to the very early cluster and buried IESs.

Supplemental Table S1. Analysis of the peaks of DNA content in all flow cytometry sorting experiments performed in this study.

Time course	Stage	PI Fluorescence Peak	Mean fluorescence (± SD)	N	CV	Range of C-value (Mbp)	Range of C-level	Estimated C-level
tc2	DEV2	tomato	458.78 ± 18.21	1154	3.97			
		new MACs	1359.06 ± 94.96	1509	6.99	5157.2-6422.4	52 - 64	~64
tc3	DEV2	tomato	583.9 ± 30.61	1922	5.24			
		new MACs, peak 1	979.07 ± 96.94	1762	9.9	2793.5-3784.5	28 - 38	~32
		new MACs, peak 2	1585.39 ± 127.26	1166	8.03	4617.5-6023.6	46 - 60	~64
tc4	DEV1	tomato	484.53 ± 21.31	1949	4.4			
		new MACs	878.66 ± 69.82	1692	7.95	3111.7-3984.6	31 - 40	~32
	DEV2	tomato	481.14 ± 20.74	1544	4.31			
		new MACs, peak 1	945.2 ± 49.49	995	5.24	3473-4204.3	35 - 42	~32
		new MACs, peak 2	1643.69 ± 98.33	1302	5.98	5992-7363.1	60 - 74	~64
	DEV3	tomato	479.92 ± 19.44	1037	4.05			
		new MACs, peak 1	1666.59 ± 103.88	629	6.2	6089.9-7482.1	61 - 75	~64
		new MACs, peak 2	2801.07 ± 218.55	3024	7.8	10064-12761	101 - 128	~128
	DEV4	tomato	479.34 ± 17.77	1134	3.71			
		new MACs	3327.55 ± 623.38	4200	18.73	10585.8-16657.3	106-167	~128
tc5	DEV1	tomato	358.59 ± 17.7	1794	4.94			
		new MACs	615.47 ± 51.65	985	8.39	2915.8-3808.3	29 - 38	~32
tc6	DEV3	tomato	569.46 ± 30.9	4324	5.43			
		new MACs	1612.44 ± 209.23	7796	12.98	4548.3-6582.3	46 - 66	~64
Aphi	DEV1	tomato	500.3 ± 28.59	2664	5.71			
		new MACs	824.06 ± 86.57	1115	9.38	2713.5-3756.7	27 - 38	~32
	DEV3 DMSO	tomato	489.86 ± 29.25	3348	5.97			
		new MACs	1639.53 ± 124.76	3223	7.61	5678.5-7453.8	57- 75	~64
	DEV3 Aphi	tomato	482.78 ± 30.2	4678	6.25			
		new MACs	878.58 ± 82.28	1794	9.36	3020.8-4131.5	30 - 41	~32

N: number of nuclei counted. CV : coefficient of variation of the DNA peaks (CV%=SD /mean fluorescence x100). The C-value and C-level for each new MAC population are estimated as described in Methods. They are presented as an interval based on the standard deviation observed for each peak distribution (tomato standard and new MACs). The last column shows the estimated C-level.

Supplemental Table S2. Sequencing data with ENA accession numbers.

Sample	ENA Accession	# of sequenced reads	# of reads mapped on the MAC	% of reads mapped on the MAC	# of reads mapped on the MIC	% of reads mapped on the MIC
FRAG (tc2)	ERS9193158	93676108	90415500	97%	92174955	98%
FRAG (tc3)	ERS9193159	77662786	74896931	96%	76186388	98%
FRAG (tc4)	ERS9193160	65870282	63439898	96%	64934908	99%
FRAG (tc5)	ERS9193161	91547362	87757956	96%	89260601	98%
32C-DEV1 (tc4)	ERS9193162	66916976	54543630	82%	65616314	98%
32C-DEV1 (tc5)	ERS9193163	78936684	60877696	77%	76636518	97%
32C-DEV2 (tc3)	ERS9193164	122760576	95220091	78%	121176641	99%
32C-DEV2 (tc4)	ERS9193165	76951432	61309368	80%	75772371	98%
64C-DEV2 (tc3)	ERS9193166	148205894	119409760	81%	145926265	98%
64C-DEV2 (tc4)	ERS9193167	74494670	61925119	83%	73833316	99%
64C-DEV2 (tc2)	ERS9193168	102849336	84030260	82%	101352683	99%
64C-DEV3 (tc6)	ERS9193169	92185998	77383722	84%	90327042	98%
64C-DEV3 (tc4)	ERS9193170	80484180	69241353	86%	79497333	99%
128C-DEV3 (tc4)	ERS9193171	54960378	50024855	91%	54345156	99%
128C-DEV4 (tc4)	ERS9193172	97332452	90725576	93%	96665100	99%
FRAG (Aphi)	ERS9193173	102454236	99678917	97%	101637829	99%
32C-DEV1 (Aphi)	ERS9193174	61535736	50774640	83%	60975841	99%
DEV3-DMSO	ERS9193175	57173842	49637234	87%	56678340	99%
DEV3-Aphi	ERS9193176	81337060	69504744	85%	80644613	99%

Supplemental Table S6. Retention statistics for several IES categories in different RNAi experiments (*PGM*, *EZL1*, *TFIIS4*, *DCL2/3* and *DCL5)*.

Category	Number	RNAi	Covered			% Not covered
			% Retained	% Not Retained	% Uncertain	
Reference IESs	44928	*PGM*	99.3	0.7	0	0
		EZL1	70.3	29.7	0	0
		TFIIS4	45.9	54.1	0	0
		DCL23	7.7	92.3	0	0
		DCL5	5.7	94.3	0	0
Internal	226	*PGM*	87.2	0	12.8	0
		EZL1	37.2	35.8	19.5	7.5
		TFIIS4	3.5	38.9	22.1	35.4
		DCL23	2.2	12.4	7.1	78.3
		DCL5	0	22.6	2.7	74.8
Internal (nested)	120	*PGM*	87.5	0	12.5	0
		EZL1	40	33.3	20.8	5.8
		TFIIS4	3.3	37.5	25.8	33.3
		DCL23	3.3	15.8	10	70.8
		DCL5	0	25	3.3	71.7
Internal (juxtaposed)	106	*PGM*	86.8	0	13.2	0
		EZL1	34	38.7	17.9	9.4
		TFIIS4	3.8	40.6	17.9	37.7
		DCL23	0.9	8.5	3.8	86.8
		DCL5	0	19.8	1.9	78.3
Encompassing	223	*PGM*	99.6	0.4	0	0
		EZL1	93.7	6.3	0	0
		TFIIS4	72.2	27.8	0	0
		DCL23	13.9	86.1	0	0
		DCL5	22.4	77.6	0	0
Internal (bigger than encompassing)	133	*PGM*	87.2	0	12.8	0
		EZL1	55.6	14.3	22.6	7.5
		TFIIS4	6	31.6	31.6	30.8
		DCL23	3.8	6	9.8	80.5
		DCL5	0	30.1	4.5	65.4
Internal (smaller than encompassing)	93	*PGM*	87.1	0	12.9	0
		EZL1	10.8	66.7	15.1	7.5
		TFIIS4	0	49.5	8.6	41.9
		DCL23	0	21.5	3.2	75.3
		DCL5	0	11.8	0	88.2
Buried	167	*PGM*	97	0	1.8	1.2
		EZL1	14.4	54.5	29.3	1.8
		TFIIS4	1.8	33.5	17.4	47.3
		DCL23	0.6	82.6	7.2	9.6
		DCL5	0	2.4	0	97.6

The first column indicates the IESs under study (reference IESs: all previously annotated IESs) and the second column indicates their numbers. The IES Retention Score (IRS) was used to determine whether an IES is retained. For IES categories “reference IESs” and “encompassing”, the previously described statistical test was used (Denby Wilkes et al. 2016). For the other categories, retention was examined only when the IES is covered by at least 10 reads ("covered IES"). Then, IESs with an IRS > 0.8 are qualified as "retained", IRS< 0.2 as "not retained" and between 0.2 and 0.8, as "uncertainly retained". The table shows the percentage of IESs falling into each category.

Supplemental References

Denby Wilkes C, Arnaiz O, Sperling L. 2016. ParTIES: a toolbox for Paramecium interspersed DNA elimination studies. *Bioinformatics* **32**: 599–601.

Dubois E, Mathy N, Regnier V, Bischerour J, Baudry C, Trouslard R, Betermier M. 2017. Multimerization properties of PiggyMac, a domesticated piggyBac transposase involved in programmed genome rearrangements. *Nucleic Acids Res* **45**: 3204–3216.

Duret L, Cohen J, Jubin C, Dessen P, Goût J-F, Mousset S, Aury J-M, Jaillon O, Noël B, Arnaiz O, et al. 2008. Analysis of sequence variability in the macronuclear DNA of Paramecium tetraurelia: a somatic view of the germline. *Genome Res* **18**: 585–596.

Lhuillier-Akakpo M, Frapporti A, Denby Wilkes C, Matelot M, Vervoort M, Sperling L, Duharcourt S. 2014. Local effect of enhancer of zeste-like reveals cooperation of epigenetic and cis-acting determinants for zygotic genome rearrangements. *PLoS Genet* **10**: e1004665.

Sellis D, Guerin F, Arnaiz O, Pett W, Lerat E, Boggetto N, Krenek S, Berendonk T, Couloux A, Aury JM, et al. 2021. Massive colonization of protein-coding exons by selfish genetic elements in Paramecium germline genomes. *PLoS Biol* **19**: e3001309.